

A Simple Stick-Slip and Creep-Slip Model for Repeating Earthquakes and its Implication for Microearthquakes at Parkfield

by N. M. Beeler, D. L. Lockner, and S. H. Hickman

Abstract If repeating earthquakes are represented by circular ruptures, have constant stress drops, and experience no aseismic slip, then their recurrence times should vary with seismic moment as $t_r \propto M_0^{1/3}$. In contrast, the observed variation for small, characteristic repeating earthquakes along a creeping segment of the San Andreas fault at Parkfield (Nadeau and Johnson, 1998) is much weaker. Also, the Parkfield repeating earthquakes have much longer recurrence intervals than expected if the static stress drop is 10 MPa and if the loading velocity V_L is assumed equal to the geodetically inferred slip rate of the fault V_f . To resolve these discrepancies, previous studies have assumed no aseismic slip during the interseismic period, implying either high stress drop or $V_L \neq V_f$. In this study, we show that a model that includes aseismic slip provides a plausible alternative explanation for the Parkfield repeating earthquakes. Our model of a repeating earthquake is a fixed-area fault patch that is allowed to continuously creep and strain harden until reaching a failure threshold stress. The strain hardening is represented by a linear coefficient C , which when much greater than the elastic loading stiffness k leads to relatively small interseismic slip (stick-slip). When C and k are of similar size creep-slip occurs, in which relatively large aseismic slip accrues prior to failure. Because fault-patch stiffness varies with patch radius, if C is independent of radius, then the model predicts that the relative amount of seismic to total slip increases with increasing radius or M_0 , consistent with variations in slip required to explain the Parkfield data. The model predicts a weak variation in t_r with M_0 similar to the Parkfield data.

Introduction

High-resolution seismological studies of faults in central California within the San Andreas fault (SAF) system reveal small repeating earthquakes with short recurrence intervals (typically $t_r < 5$ yr). These earthquakes occur on different faults in a number of locations, including an $M \sim 1.5$ earthquake sequence on the Calaveras fault in the aftershock zone of the 1984 Morgan Hill earthquake (Vidale *et al.*, 1994; Marone *et al.*, 1995), six $M \sim 1.5$ earthquake sequences in the aftershocks of the 1989 Loma Prieta earthquake (Schaff *et al.*, 1998), 53 $M < 1.5$ earthquake sequences in the Parkfield segment (Nadeau and Johnson, 1998), and 37 sequences on the Hayward fault from north of El Cerrito south to San Leandro (Burgmann *et al.*, 2000). Study of small earthquakes with short recurrence may provide insight into the behavior of larger repeating earthquakes, which are of greater interest because of their greater damage potential, but are more difficult to study because they have longer repeat times. However, for these particular small events, scaling of source parameters to the size appropriate for hazardous earthquakes is controversial; for example the variation of recurrence interval with seismic moment M_0 for the Park-

field repeating earthquakes of Nadeau and Johnson (1998) is weaker than expected based on standard assumptions (Fig. 1). To illustrate, we calculate the expected relationship between recurrence and seismic moments for a circular rupture assuming no aseismic creep and constant stress drop, as might be expected for large earthquakes. Here we have used the static stress drop for a circular patch of radius r ,

$$\Delta\tau_s = \frac{7\pi\mu\Delta\delta_{\text{seis}}}{16r} \quad (1a)$$

(Eshelby, 1957; Keilis-Botok, 1959), and the standard definition of seismic moment

$$M_0 = \mu\pi r^2 \Delta\delta_{\text{seis}}, \quad (1b)$$

where μ is the shear modulus. Assuming that the total slip over the seismic cycle is the seismic slip $\Delta\delta_{\text{total}} = \Delta\delta_{\text{seis}} = t_r V_L$, we find

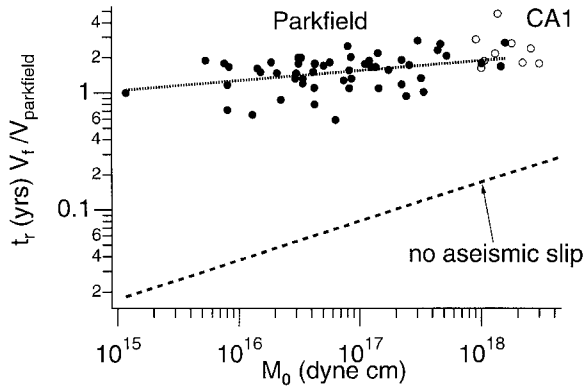


Figure 1. Repeating earthquake recurrence. Solid symbols are for Parkfield sequences from Nadeau and Johnson (1998). Recurrence interval was determined from published values of average moment and moment rate $t_r = M_0/M_0$. The dotted line is a linear least-squares fit with slope 0.086. Open symbols are for the CA1 sequence of Vidale *et al.* (1994). Recurrence and seismic moment for CA1 were determined as described in the text. The dashed reference line is the expected scaling of t_r with M_0 from a circular rupture assuming constant stress drop and no aseismic slip (see text).

$$t_r = \frac{\Delta\tau_s^{2/3} M_0^{1/3}}{1.81\mu V_L}, \quad (2)$$

where V_L is loading velocity. Thus, if stress drop is constant, $t_r \propto M_0^{1/3}$, a variation with moment significantly stronger than observed for the Parkfield repeating earthquakes (Fig. 1); a least-squares fit to the data gives $t_r \propto M_0^{-1/11}$ (dotted line, Fig. 1). In addition, using equation (2), a constant stress drop of 10 MPa, and loading velocity $V_L = V_f = 2.3$ cm/yr, the average creep rate of the SAF at Parkfield (Nadeau and Johnson, 1998), we find that the observed recurrence intervals are longer than expected by almost two orders of magnitude for the smallest events and by a factor of 10 for the largest events.

To explain the discrepancies between the expected and observed recurrence intervals (Fig. 1) Nadeau and Johnson (1998) assumed no aseismic slip during the interseismic period and constant V_L . Using these assumptions with equation (1a) and (1b) leads to

$$\Delta\tau_s = 2.44 \frac{(t_r V_L \mu)^{3/2}}{\sqrt{M_0}}. \quad (3)$$

Thus, because recurrence for the Parkfield repeating sequences is approximately independent of seismic moment (Fig. 1), based on these assumptions, the stress drop inferred by Nadeau and Johnson (1998) decreases with moment (Fig. 2). This scaling with moment is qualitatively consistent with laboratory scaling of rock strength with sample size. However, using equation (3) and $V_L = V_f$, Parkfield repeating

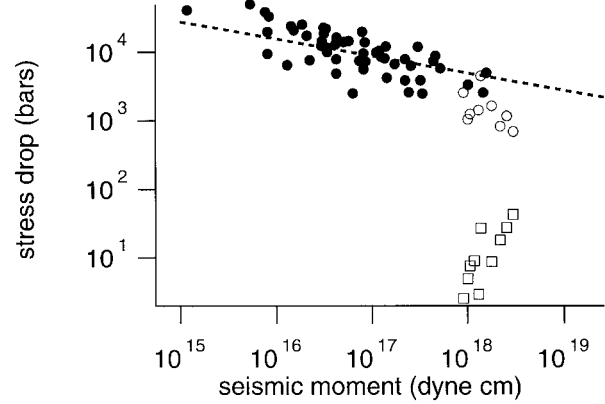


Figure 2. Repeating earthquake stress drop. Solid symbols are for the Parkfield sequences of Nadeau and Johnson (1998), using their procedure for calculating stress drop; they assume no aseismic slip and a loading rate equal to the average creep rate of the San Andreas fault at Parkfield. The open symbols are for the CA1 sequence of Vidale *et al.* (1994). Two estimates for CA1 are shown. High stress drops are estimated for CA1 if the procedure of Nadeau and Johnson (1998) is followed (open circles). Lower and more typical (<16 MPa) stress drops are found for CA1 if rupture duration of Vidale *et al.* (1994) is used (open squares) (see text). The diagonal line is the scaling relation for stress drop with seismic moment proposed by Nadeau and Johnson (1998).

events have inferred $\Delta\tau_s = 250\text{--}5000$ MPa, which is very much larger than typical for earthquakes, for example, $\Delta\tau_s = 2.0 \times 10^{-2}$ to 60 MPa for events with $-1 \leq M_L \leq 5$ (Abercrombie, 1995a,b), and the implied fault strength, even assuming complete stress drop, is higher than typical laboratory rock strength (see summary in Lockner, 1995).

Do small repeating earthquakes on strike-slip faults in central California have high stress drop? While the stress drops of repeating events at Parkfield are unconstrained, stress drop of other similar repeating earthquake sequences, such as CA1 (Vidale *et al.*, 1995), are better defined. The CA1 repeating earthquake ($M \sim 1.5$) is located along the Calaveras fault south of the epicenter of the 1984 Morgan Hill earthquake (Vidale *et al.*, 1994; Marone *et al.*, 1995). Rapid creep (afterslip) was induced in this fault segment by stress transfer from the Morgan Hill mainshock (Ellsworth, 1995). To compare CA1 with the Parkfield sequences, we first estimate the CA1 loading rate from fault creep (12–0.8 mm/day for the period May–August 1984) (Prescott *et al.*, 1986) inferred from length changes of the Hamilton to Llagas geodetic line, which crosses the fault obliquely. To compare recurrence between regions with different loading rates we use the expectation that recurrence and loading velocity are inversely related to first order (e.g., Beeler *et al.*, 2001) and normalize recurrence by the ratio of the loading rate to the Parkfield loading rate (also see Nadeau and McEvilly, 2000). The CA1 relative moments M_r of Vidale *et al.* (1994)

were converted to seismic moment assuming a mean event magnitude of M 1.5 ($M = 1.5M_r$) and the relationship $M_0 = 10^{1.5M+16.1}$ (Hanks and Kanamori, 1979) where M_0 is in units of dyne cm. We restrict our attention to events subsequent to the Morgan Hill earthquake on 24 April 1984 and prior to the occurrence of a nearby M 1.4 earthquake on 19 February 1985, which induced a significant static stress change on the CA1 source region (Ellsworth, 1995). After accounting for the large differences in loading rate, the CA1 sequence can be seen to have the same kind of anomalous, long recurrence intervals as the Parkfield repeating events; the CA1 sequence recurrence, when plotted versus seismic moment, are on trend with recurrence of the Parkfield repeating earthquakes (Fig. 1). A result of the consistency of recurrence between the Parkfield events and the CA1 sequence is that when the CA1 stress drops are estimated using equation (3), stress drop is also on trend with the Parkfield data (Fig. 2).

However, stress drop for CA1 is constrained by the event duration t_d , equivalent to the reciprocal of the corner frequency, which was estimated for the CA1 sequence using spectral techniques by Vidale *et al.* (1994). We convert the event duration (Vidale *et al.*, 1994) to rupture radius assuming a Brune source model with rupture velocity $V_r = 0.9\beta$ (β is the shear-wave speed) yielding the duration $t_d = 2.4r/V_r$. The stress drop is calculated from seismic moment using equation (1a) and (1b), which yields $\Delta\tau_s = 6.04M_0/(t_d V_r)^3$. Using these assumptions and $V_r = 2.5$ km/sec, we find $\Delta\tau_s < 16$ MPa for CA1 (Fig. 2), inconsistent with the inferred stress drop for Parkfield events. While our finding of lower stress drop for CA1 does not pertain directly to stress drops for the Parkfield repeating earthquakes, because the Parkfield sequences are but one set of many sequences that show anomalous long recurrence (Nadeau and McEvilly, 2000), our finding for CA1 indicates that small repeating earthquakes generally do not have high stress drop. Furthermore, preliminary event duration-based estimates for selected same-locale M_w 1.1–5.0 earthquakes at Parkfield find stress drops of 1.0–50 MPa (Johnson and Dreger, 2000), consistent with CA1.

One alternative to the high-stress-drop model for repeating earthquakes is to reduce the loading rate by shielding the repeating events with adjacent locked regions (Anooshpoo and Brune, 2001; Sammis and Rice, 2001); a second alternative, which we develop in this article, is to allow significant aseismic slip during the interseismic period (oral presentation, Ellsworth *et al.*, 1998). Fault patches that sustain significant aseismic creep prior to failure are observed during laboratory failure cycles, for example in clay-rich fault gouges (Morrow *et al.*, 1982) and serpentinites (Summers and Byerlee, 1977). Figure 3 shows repeating stress drop following large amounts of aseismic creep (the ratio of seismic to total slip $R \approx 0.25$) for serpentinite at room temperature and 150 MPa confining pressure (Summers and Byerlee, 1977). Although there is presently no theory to account for this creep-slip behavior in room temperature lab-

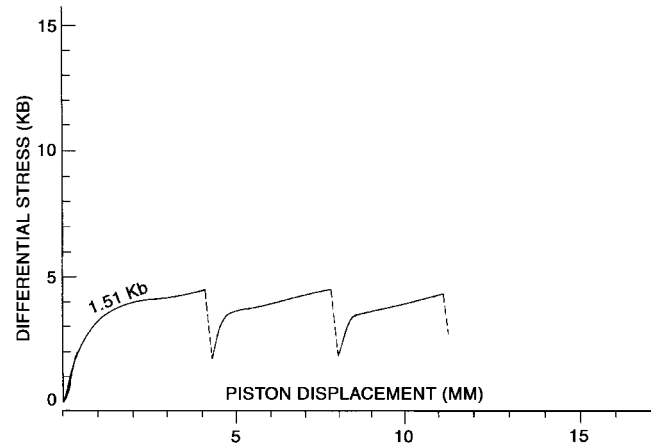


Figure 3. Apparent creep-slip in a laboratory experiment (Summers and Byerlee, 1977). The experiment was conducted on a 0.025-in. thick wafer of dry serpentinite sheared between granite blocks at a strain rate of 10^{-4} per sec at 150 MPa confining pressure. The differential stress is the difference between the confining pressure and the greatest principal stress. The horizontal axis is the displacement of the loading piston that increases the greatest principal stress and the shear stress on the fault at a rate $d\tau/d\delta_l = k$, so long as the fault is not sliding. The periods in which the stress increases rapidly with piston displacement correspond to elastic loading with slope proportional to the machine stiffness k . The periods in which the stress increases weakly with piston displacement are periods of ongoing fault creep. The periodic stress drops are the laboratory equivalent of repeating earthquake stress drop.

oratory experiments, it is expected at natural conditions, albeit under restrictive circumstances. For example, Sleep and Blanpied (1992) suggest that porous, ductile faults will shear and compact simultaneously under increasing tectonic load. Compaction will increase the density and hence the resistance to further shearing, equivalent to the shear stress on the fault plane τ ; if the fault zone is undrained, compaction will also increase the pore fluid pressure p . Under such conditions the shear stress will increase, and the effective stress can decrease with time during loading until a brittle, frictional failure strength is reached and seismic stress drop occurs. Although ductile fault zones in the Sleep and Blanpied model are intended to deform via high-temperature solution-aided creep (pressure solution), this model can be adapted to more general situations (cf. Fig. 3). We define a material as ductile if it is capable of sustaining permanent deformation without loss of strength (regardless of the deformation mechanism) and note that the requirements for creep-slip are simply an initially ductile fault zone that strain hardens. During continuous tectonic loading, such a material will eventually reach a ductile limit at high stress and become brittle (where strength loss accompanies continued permanent deformation). This conceptual model may be appropriate for small repeating earthquakes (Vidale *et al.*, 1994; Marone *et al.*, 1995; Nadeau and Johnson, 1998; Schaff *et al.*, 1998;

Burgmann *et al.*, 2000), which occur exclusively in creeping (ductile) sections of faults—regions where most of the total moment is released in aseismic fault slip (e.g., Wesson *et al.*, 1973).

In this article we develop a simple model, based crudely on the experiments and theoretical results cited previously. The model is intended to be simple so that analytical expressions for source properties can be derived and applied to observational data. The model, which predicts relationships between seismic slip, aseismic slip, stress drop, earthquake recurrence, and seismic moment, is tested against the Parkfield repeating microearthquake catalog.

Model

For small repeating-earthquake sequences, failure is thought to occur on a single asperity or fault patch embedded in an aseismically creeping fault plane (Vidale *et al.*, 1994; Ellsworth, 1995; Marone *et al.*, 1995; Nadeau and Johnson, 1998; Nadeau and McEvilly, 1999) (Fig. 4). In this case, recurrence is apparently controlled by the rate of aseismic creep of the fault surrounding the patch, as geodetically measured fault creep correlates with cumulative earthquake moment release rate and with recurrence interval (e.g., Ellsworth, 1995; Beeler *et al.*, 2001). To represent this behavior we consider a fault plane containing a circular patch with radius r . The fault patch represents a region with material properties that are somewhat different than the fault surrounding the patch (surroundings). The fault surrounding the patch has homogeneous material properties that allow aseismic slip at a constant shear resistance. Stress on the patch is assumed uniform or can be well characterized by a spatial average. Loading of the patch occurs by elastic stress transfer from the creeping part of the fault plane to the patch, and can be represented by

$$\tau = k(\delta_L - \delta_{\text{aseis}}) = k(\delta_{L0} + V_L t - \delta_{\text{aseis}}), \quad (4)$$

where the stiffness $k \propto 1/r$, δ_{aseis} is the interseismic displacement of the patch, and δ_L , δ_{L0} , and V_L are the displacement, the initial displacement, and the slip velocity of the surroundings, respectively. If the long-term slip rate of the fault patch and the long-term slip rate of the surroundings are equivalent (i.e., $\Delta\delta_L = \Delta\delta_{\text{total}} = \Delta\delta_{\text{seis}} + \Delta\delta_{\text{aseis}}$), and the patch radius is constant, then $k = \Delta\tau_s / \Delta\delta_{\text{seis}}$ (see Appendix). Here, $\Delta\delta_{\text{seis}}$ is the spatial average of seismic slip over the patch during a single earthquake.

We desire a fault-strength relation for the patch that allows for interseismic slip. This requirement is met if patch strength prior to failure is an increasing function of fault slip, that is, a slip- or strain-hardening behavior (e.g., Morrow *et al.*, 1982)

$$\tau_{\text{strength}} = \tau_o + C\delta_{\text{aseis}}, \quad (5)$$

where the slip-hardening coefficient $C = d\tau_{\text{strength}}/d\delta_{\text{aseis}}$ is a positive constant and τ_o (residual stress) is the strength at

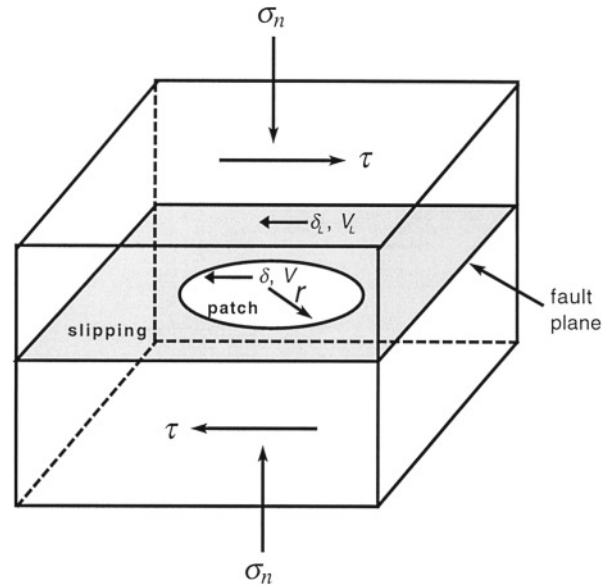


Figure 4. Geometry of a simple creep-slip model consisting of a circular seismic patch of radius r embedded in an elsewhere aseismic creeping fault plane. Slip and slip velocity of the creeping fault surrounding the patch are δ_L and V_L , respectively. The slip and slip velocity of the patch during loading are δ and V , respectively.

the onset of the loading cycle. The patch slips continuously during loading, possibly at an extremely low rate, thus fixing the shear stress $\tau = \tau_{\text{strength}}$. Noting that $\tau = k\delta_{L0}$ from equations (4) with (5) we have

$$\delta_{\text{aseis}} = \frac{kV_L t}{(C+k)}, \quad (6a)$$

and

$$\tau = \tau_o + C \left(\frac{kV_L t}{(C+k)} \right). \quad (6b)$$

If the loading rate is constant, we can determine the sliding rate during loading by equating the time derivatives of equations (4) and (5) to obtain:

$$V = \frac{kV_L}{C+k}. \quad (6c)$$

We then assume that seismic failure occurs when τ reaches a threshold strength τ_f , and stress immediately drops to τ_o , thereby defining the static stress drop $\Delta\tau_s = \tau_f - \tau_o$. We assume that the patch constitutive behavior follows equation (6) over multiple loading cycles; thus we implicitly assume that earthquake stress drop resets the patch strength and does not alter the constitutive behavior in subsequent loading cycles. From equation (6b) the earthquake recurrence interval is given by

$$t_r = \frac{\Delta\tau_s}{V_L} \left(\frac{1}{k} + \frac{1}{C} \right). \quad (7)$$

To determine the ratio of seismic to total slip R we use the seismic slip resulting from elastic unloading of the fault, given by $\Delta\delta_{\text{seis}} = \Delta\tau_s/k$, and the total slip $\Delta\delta_{\text{total}} = V_L t_r$. Combining these definitions with equation (7) leads to

$$R = \frac{\Delta\delta_{\text{seis}}}{\Delta\delta_{\text{total}}} = \frac{1}{(1+k/C)}. \quad (8)$$

Note that R is not directly dependent on loading velocity or stress drop.

Stick-slip. Stick-slip behavior occurs when $k \ll C$. In this case, equation (6b) is

$$\tau \approx \tau_o + kV_L t, \quad (9a)$$

equation (7) becomes

$$t_r \approx \frac{\Delta\tau_s}{kV_L}, \quad (9b)$$

and equation (6c) is

$$V \approx \frac{kV_L}{C}. \quad (9c)$$

Equations (9a) and (9b) are the same as expected from constant-velocity loading of a fault with a truly static strength threshold (e.g., Beeler *et al.*, 2001) because, though fault creep occurs during loading, the net creep is negligible compared with the seismic slip, that is, from equation (8) $R \approx 1$.

Aseismic slip. When $k \gg C$ the fault can be effectively aseismic. In this case, equation (6b) is

$$\tau \approx \tau_o + CV_L t, \quad (10a)$$

equation (7) becomes

$$t_r \approx \frac{\Delta\tau_s}{CV_L}, \quad (10b)$$

and equation (6c) is

$$V \approx V_L. \quad (10c)$$

Provided k is small, as is expected in the Earth (e.g., Walsh, 1971), and since $k \gg C$, C is smaller still, and from equation (10a), $\tau \approx \tau_o$. In other words, the shear stress is effectively fixed at a constant yield stress. The recurrence interval (equation [10b]) then becomes infinite, the interseismic slip velocity is nearly equal to the velocity of the surrounding fault plane, and $R \approx 0$.

Creep-slip. Creep-slip occurs when k and C are of similar magnitude. In this case considerable fault creep, relative to seismic slip, occurs prior to failure, and τ , t_r , and V are given by the general relations equations (6b), (7), and (6c).

Implications: Parkfield Microearthquakes

To further illustrate the range of responses expected from equation (6b), consider repeating earthquakes with a wide range of r . Combining equations (1a) and (1b) we find $k = 1.81\mu(\Delta\tau_s/M_0)^{1/3}$, and combining this result with equation (8), the ratio of stress drop to seismic slip of a circular fault patch is

$$R = \frac{1}{\left(1 + \frac{1.81\mu}{C} \left[\frac{\Delta\tau_s}{M_0} \right]^{1/3} \right)}. \quad (11)$$

Presuming that C is constant, large-moment events have $R \approx 1$, and small events have $R \approx 0$ (Fig. 5a). For small events, the value of R from equation (11) approaches 0 as a power law

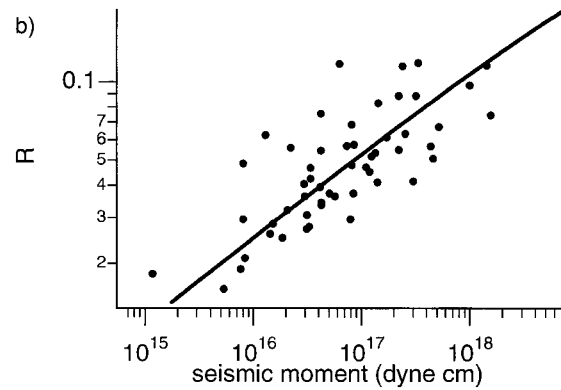
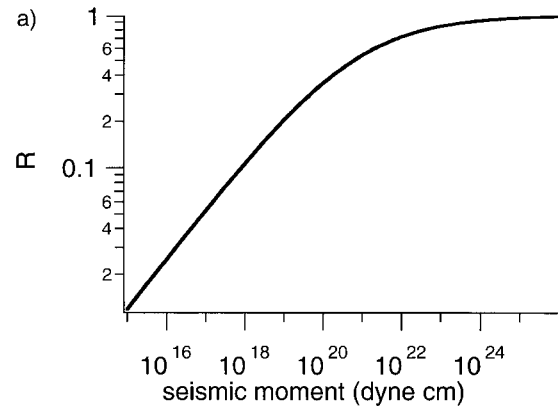


Figure 5. Comparison of the ratio of seismic to total slip R from the creep-slip model and as estimated for the Parkfield data. (a) R , equation (11) with $C = 3.0$ MPa/cm, $\Delta\tau_s = 10$ MPa, $\mu = 3 \times 10^{11}$ dyne/cm², and $V_L = 2.3$ cm/yr. (b) Parkfield data assuming constant stress drop, equation (13). The line is R calculated from the creep-slip model (equation [11]) using the same parameters as in (a).

$$R \approx \frac{C}{1.81\mu} \left[\frac{M_0}{\Delta\tau_s} \right]^{1/3}. \quad (12)$$

This is a scaling relation for slip with earthquake size considered unlikely by Nadeau and Johnson (1998), and the power law exponent (the slope in Fig. 5a) is independent of loading rate, stress drop, and the strain hardening rate for small events.

Now we consider estimated values of R for the 53 repeating microearthquake sequences at Parkfield compiled by Nadeau and Johnson (1998). We assume that $\Delta\tau_s$, V_L , and C are constants and that all ruptures are circular. Using equations (1a) and (1b), the ratio of seismic slip to total slip is

$$R = 0.55 \frac{\Delta\tau_s^{2/3} M_0^{1/3}}{V_L t_r \mu}. \quad (13)$$

As recurrence for the Parkfield sequences is largely independent of seismic moment (Fig. 1), equation (13) requires a systematic increase of R with moment. Assuming $\Delta\tau_s = 10$ MPa and $V_L = V_f = 2.3$ cm/yr, we use equation (13) to estimate R for the Parkfield sequences (Fig. 5b), and find the Parkfield events are consistent with our creep-slip model if $C = 3$ MPa/cm. However, this comparison between model-predicted and inferred R assumes constant stress drop for the Parkfield microearthquakes, which is debatable.

A fairer assessment of the model is a comparison between observed recurrence interval (Fig. 1) and model predictions. Using the circular patch stiffness, as derived from equations (1a) and (1b) previously, in equation (7) we have

$$t_r = \frac{\Delta\tau_s}{V_L} \left(\frac{1}{1.81\mu} \left[\frac{M_0}{\Delta\tau_s} \right]^{1/3} + \frac{1}{C} \right) \quad (14)$$

(see Fig. 6a). At large seismic moments $t_r \propto M_0^{1/3}$; thus t_r continues to increase with increasing moment as a power law, a result identical to the expectation based on no aseismic slip (see Fig. 1). At small seismic moments $t_r \approx \Delta\tau_s / CV_L$ and, since C , $\Delta\tau_s$, and V_L are assumed constant, t_r is independent of moment. Figure 6b compares the Parkfield observations with the calculated variation of t_r with M_0 for two choices of loading velocity. The loading velocity (the subsurface creep rate of the SAF) for the Parkfield earthquake sequences is expected to vary spatially between 0.4 and 3.5 cm/yr (Nadeau and Johnson, 1998 after Harris and Segall, 1987); so, we calculate two predictions corresponding to these rates for $C = 3.0$ MPa/cm and $\Delta\tau_s = 10$ MPa. These representations bound the data fairly well, and the Parkfield data suggest that t_r is weakly dependent on moment at low M_0 as required by the model, although the scatter in the data is considerable.

Discussion

Whereas our calculations with equation (6b) argue for creep-slip as a plausible explanation of the Parkfield repeat-

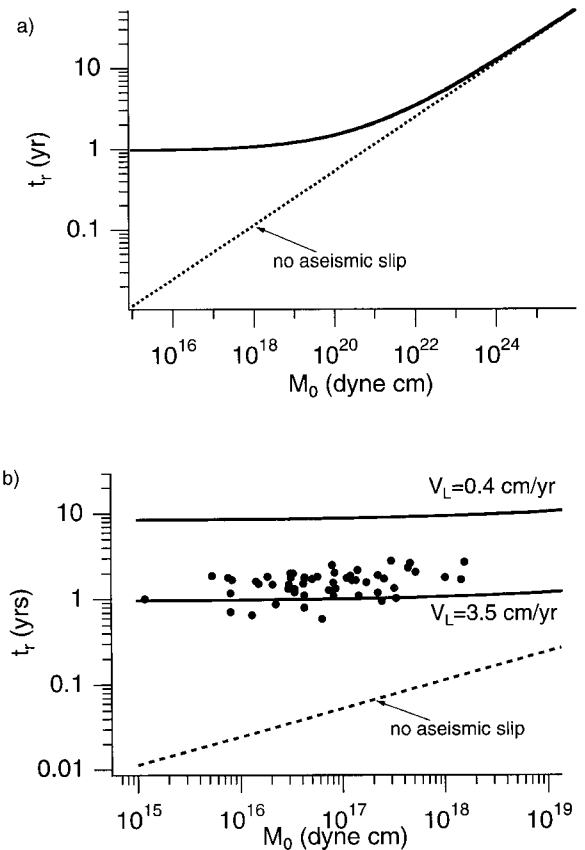


Figure 6. Comparison of t_r predicted by the creep-slip model with the Parkfield data. (a) t_r , equation (14) with $C = 3.0$ MPa/cm, $\Delta\tau_s = 10$ MPa, $\mu = 3 \times 10^{11}$ dyne/cm², and $V_L = 2.3$ cm/yr. (b) Parkfield data and predictions of the creep-slip model using the same parameters as in (a). Two choices of loading velocity are shown, which represent the limits of estimated subsurface creep rate appropriate for the Parkfield segment (Harris and Segall, 1987; Nadeau and Johnson, 1998). The reference line in parts (a) and (b) is the same as the dashed line in Figure 1, corresponding to equation (2) using the parameters listed in Figure 6a.

ing-event source properties, the strain-hardening rate where creep-slip is observed in the laboratory is much larger (e.g., in Fig. 3 $C = 309$ MPa/cm) than required to fit the Parkfield data with 10 MPa stress drop ($C = 3$ MPa/cm). As creep-slip occurs when k and C are of similar magnitude, the value of C used to model the seismic observations would result in only aseismic creep in the laboratory (i.e., $k \gg C$) simply because laboratory stiffness is higher than the patch stiffness of a small earthquake ($k = 239\text{--}0.11$ MPa/cm for Parkfield events assuming $\Delta\tau_s = 10$ MPa). For example, using $k = 5 \times 10^2$ MPa/cm, as appropriate for laboratory experiments, $V_L = 0.1$ μ m/sec, $\Delta\tau_s = 10$ MPa, and $C = 3$ MPa/cm in equations (7) and (8) we find $R = 0.006$ and $t_r = 3.35 \times 10^5$ sec. This recurrence interval exceeds the duration of most laboratory tests; thus multiple stick-slip cycles (as observed in Fig. 3) would not be expected in the lab for these

parameter values. Furthermore, the total cycle displacement (3.3 cm) predicted by $C = 3$ MPa/cm exceeds the limit of most testing machines (e.g., Fig. 3). Thus, while creep-slip is observed in the laboratory, scaling to earthquake dimensions is not currently understood, and the strain-hardening rates implied by the Parkfield sequences are not presently validated by laboratory measurements. It is also worth noting that the laboratory observations indicate a more complicated nonlinear strain hardening than the simplified linear strain hardening used in our model. A more realistic creep-slip model, one whose strain-hardening rate is controlled by an underlying physical mechanism, would be preferable to equation (6b).

Previous studies have suggested simple scaling relationships between the source parameters of small and large repeating earthquakes; for example, a scaling relation between static stress drop and seismic moment has been proposed by Nadeau and Johnson (1998) (Fig. 2). Whereas the results of the present study could be used to extrapolate t_r and R to larger events (Figs. 5a and 6a), this is not recommended. Laboratory observations indicate a wide range of possible fault strengths (e.g., Morrow *et al.*, 1982, 2000), and a wide range of responses to stressing is expected to result from variations in fault zone mineralogy alone. Even assuming the creep-slip model equation (6b) is relevant to all repeating earthquakes, it would be unwise to expect C to be spatially constant for all fault segments within the San Andreas system; possibly C should not even be treated as a constant within the Parkfield segment, as we have done. It is also unlikely that stress drops are constant for all earthquakes (Abercrombie, 1995a,b), as we have assumed. However, our simple creep-slip model does reproduce the systematic variation in source properties with moment that is required by the Parkfield observations.

Dichotomous classification of natural faults and fault segments into aseismic or seismic may be too restrictive. When examined at high enough resolution, laboratory faults, even those that stick-slip, undergo precursory aseismic slip. In the case of undercompacted gouges layers, which may have porosity that resembles natural faults following stress drop (e.g., Sleep and Blanpied, 1992), large amounts of strain-hardening and aseismic slip can occur during initial loading (Lockner, unpublished data). Thus laboratory-based distinctions between aseismic slip (stable sliding) and stick-slip (unstable sliding) are not simple, and intermediate behavior is possible (e.g., Fig. 3). Could earthquakes creep-slip? Our analysis of the Parkfield events suggest this possibility, but the source parameters of these events are not well constrained and our explanation is not definitive (Nadeau and Johnson, 1998; Anooshpoo and Brune, 2001; Sammis and Rice, 2001).

Conclusions

Small seismic fault patches could sustain relatively large amounts of aseismic creep during the interseismic pe-

riod if such patches are ductile at low stress, strain harden, and eventually experience brittle failure at higher stress. Under these circumstances, if the stress drop is constant, the ratio of seismic to total slip R increases with moment as $R \propto M_o^{1/3}$, matching variations in aseismic slip required to explain small repeating earthquake sequences at Parkfield. For such faults that strain harden prior to earthquake failure, small event recurrence interval is expected to be weakly dependent on event size, as is observed for the Parkfield microearthquakes.

Appendix: Fault Patch Slip Budget

Consider the slip budget for a fault patch embedded in and loaded by creep of the surrounding fault plane (Fig. 4). Over one period of the seismic cycle the total slip

$$\Delta\delta_{\text{total}} = \Delta\delta_{\text{seis}} + \Delta\delta_{\text{aseis}}, \quad (\text{A1})$$

where $\Delta\delta_{\text{seis}}$ and $\Delta\delta_{\text{aseis}}$ are the spatial averages over the patch of seismic slip and aseismic slip, respectively. During loading to failure, creep δ_L of the surrounding fault plane elastically transfers stress to the patch through a loading stiffness $k_L = d\tau/d\delta_L$, representing the spatially averaged stress change over the patch per increment of loading. The patch loading stiffness k_L depends on the size of the fault patch. If the fault patch itself slips during loading, stress is relieved according to a displacement rate of unloading $k_u = d\tau/d\delta_{\text{aseis}}$ representing the spatially averaged stress change per increment of slip of the patch, which also depends on the size of the patch. For loading from a residual stress τ_o to a failure stress τ_f we then have

$$\Delta\tau_s = \tau_f - \tau_o = k_L\Delta\delta_L - k_u\Delta\delta_{\text{aseis}}, \quad (\text{A2})$$

where $\Delta\delta_L$ is the total creep displacement of the fault surrounding the patch during the loading cycle. Noting that the duration of earthquake stress drop is extremely short with respect to the duration of the loading cycle, $\Delta\delta_L$ is equivalent to the total slip of the surroundings over the earthquake cycle. We assume that over a single period of the seismic cycle, total slip of the patch is equal to the total slip of the creeping surroundings

$$\Delta\delta_{\text{total}} = \Delta\delta_L. \quad (\text{A3})$$

In other words, the long-term creep rate of the fault and the long-term slip rate on the patch are equivalent so that there is no long-term slip deficit or, conversely, any excess seismic-moment release. The static stress drop $\Delta\tau_s$ is also related to the fault slip through the displacement-averaged unloading stiffness;

$$\Delta\tau_s = k_u\Delta\delta_{\text{seis}}. \quad (\text{A4})$$

Substituting for $\Delta\tau_s$ from equation (A4) and for $\Delta\delta_L$ from equation (A3) into equation (A2) we have

$$\Delta\delta_{\text{total}} = \frac{k_u}{k_L} (\Delta\delta_{\text{seis}} + \Delta\delta_{\text{aseis}}). \quad (\text{A5})$$

By combining equations (A1) and (A5), we find $k_L = k_u$; we use a single value of stiffness $k = k_L = k_u$ throughout this article.

Acknowledgments

Discussions between NMB and Bill Ellsworth led directly to the results presented in this article. Other discussions with D. Schaff, G. Beroza, B. Nadeau, A. McGarr, and A. Michael are gratefully acknowledged. B. Ellsworth, J. Gombert, A. Michael, G. Bokelmann, C. Sammis, an anonymous referee, and the associate editor S. Day provided comments that improved the manuscript.

References

- Abercrombie, R. E. (1995a). Earthquake source scaling relationships from -1 to $5 M_L$ using seismograms recorded at 2.5 km depth, *J. Geophys. Res.* **100**, 24,015–24,036.
- Abercrombie, R. E. (1995b). Earthquake locations using single station deep borehole recordings: implications for microseismicity on the San Andreas Fault in southern California, *J. Geophys. Res.* **100**, 24,003–24,014.
- Anooshehpour, A., and J. N. Brune (2001). Quasi-static slip-rate shielding by locked and creeping zones as an explanation for small repeating earthquakes at Parkfield, *Bull. Seism. Soc. Am.* **91**, 401–403.
- Beeler, N. M., S. H. Hickman, and T.-f. Wong, (2001). Earthquake stress drop and laboratory-inferred interseismic strength recovery, *J. Geophys. Res.* (in press).
- Burgmann, R., D. Schmidt, R. M. Nadeau, M. d'Alessio, E. Fielding, D. Manaker, T. V. McEvilly, and M. H. Murray (2000). Earthquake potential along the Northern Hayward Fault, California, *Science* **289**, 1178–1182.
- Ellsworth, W. L. (1995). Characteristic earthquakes and long-term earthquake forecasts: implications of central California seismicity, in *Urban Disaster Mitigation: the Role of Science and Technology*, F. Y. Cheng and M. S. Sheu (Editors), Elsevier, Amsterdam, 1–14.
- Ellsworth, W. L., A. T. Cole, L. D. Dietz, and D. A. Dodge (1998). Repeating earthquakes and the longterm evolution of seismicity on the San Andreas Fault near Bear Valley, California, *Seism. Res. Lett.* **69**, 144.
- Eshelby, J. D. (1957). The determination of the elastic field of an ellipsoidal inclusion, and related problems, *Proc. R. Soc. Lond. A.* **241**, 376–396.
- Hanks, T. C., and H. Kanamori (1979). A moment magnitude scale, *J. Geophys. Res.* **84**, 2348–2350.
- Harris, R. A., and P. Segall (1987). Detection of a locked zone at depth on the Parkfield, California, segment of the San Andreas Fault, *J. Geophys. Res.* **92**, 7945–7962.
- Johnson, P. A. B., and D. S. Dreger (2000). Source process times and slip distribution of Parkfield earthquakes M 1 to 5, *Seism. Res. Lett.* **71**, 263.
- Keilis-Borok, V. I. (1959). On estimation of the displacement in an earthquake source and of source dimension, *Ann. Geofis.* **12**, 205–214.
- Lockner, D. A. (1995) Rock failure, in *Rock Physics and Phase Relations, A Handbook of Physical Constants*, American Geophysical Union, Washington, D.C., 127–147.
- Marone, C., J. E. Vidale, and W. L. Ellsworth (1995). Fault healing inferred from time dependent variations in source properties of repeating earthquakes, *Geophys. Res. Lett.* **22**, 3095–3098.
- Morrow, C. A., D. E. Moore, and D. A. Lockner (2000). The effect of mineral bond strength and adsorbed water on fault gouge frictional strength, *Geophys. Res. Lett.* **27**, 815–818.
- Morrow, C. A., L. Q. Shi, and J. D. Byerlee (1982). Strain hardening and strength of clay-rich fault gouges, *J. Geophys. Res.* **87**, 6771–6780.
- Nadeau, R. M., and L. R. Johnson (1998). Seismological studies at Parkfield VI: moment release rates and estimates of source parameters for small repeating earthquakes, *Bull. Seism. Soc. Am.* **88**, 790–814.
- Nadeau, R. M., and T. V. McEvilly (1999). Fault slip rates at depth from recurrence intervals of repeating microearthquakes, *Science* **285**, 718–721.
- Nadeau, R. M., and T. V. McEvilly (2000). Spatial and temporal heterogeneity of fault slip on the San Andreas Fault system in central California, *Seism. Res. Lett.* **71**, 263.
- Prescott, W. H., N. E. King, and G. Guohua (1986). Preseismic, coseismic and postseismic deformation associated with the 1984 Morgan Hill, California, earthquake, in *The 1984 Morgan Hill California Earthquake*, J. H. Bennett and R. W. Sherburne (Editors), California Division of Mines and Geology Special Publication 68, 137–148.
- Sammis, C. G., and J. R. Rice (2001). Repeating earthquakes as low-stress drop events at a border between locked and creeping fault patches, *Bull. Seism. Soc. Am.* **91**, 532–537.
- Schaff, D. P., G. C. Beroza, and B. E. Shaw (1998). Postseismic response of repeating aftershocks, *Geophys. Res. Lett.* **25**, 4559–4552.
- Sleep, N. H., and M. L. Blanpied (1992). Creep, compaction and the weak rheology of major faults, *Nature* **359**, 687–692.
- Summers, R., and J. Byerlee (1977). Summary of results of frictional sliding studies, at confining pressures up to 6.98 kb, in select rock materials, *U.S. Geol. Surv. Open-File Rept. 77-142*, 129 pp.
- Vidale, J. E., W. L. Ellsworth, A. Cole, and C. Marone (1994). Rupture variation with recurrence interval in 18 cycles of a small earthquake, *Nature* **368**, 624–626.
- Walsh, J. B. (1971). Stiffness in faulting and in friction experiments, *J. Geophys. Res.* **76**, 8597–8598.
- Wesson, R. L., R. O. Burford, and W. L. Ellsworth (1973). Relationship between seismicity, fault creep and crustal loading along the central San Andreas Fault, Stanford University Publications, Geological Sciences, Vol. 13, 303–321.
- U.S. Geological Survey
Menlo Park, California

Manuscript received 23 June 2000.